THE AXIALLY ROTATING SEGMENTED ROD

C. Y. WANG

Departments of Mathematics and Mechanical Engineering, Michigan State University,
Wells Hall, East Lansing, MI 48824-1027, U.S.A.

Abstract—A rod, composed of N rigid segments and N torsion springs at the joints, is rotated axially from one end. The equilibrium shape is governed by a nonlinear difference equation with a parameter B signifying the relative importance of centrifugal forces to the restoring forces of the springs. Linear analysis yields the eigenspeeds B_c from which nontrivial solutions bifurcate. The nonlinear problem is solved numerically.

1. INTRODUCTION

It has long been known that axially rotating rods become unstable when certain critical angular speeds are reached (Love, 1944). The existence of the bifurcation solutions for an elastic rod axially rotated from one end was discussed by Odeh and Tadjbakhsh (1965). The nonlinear bifurcation solutions were integrated by Wang (1982) and estimated by Atanackovic (1984).

The present paper studies the rotation of a segmented rod which has never been considered before. Rotating segmented rods occur in many instances including drill strings of off-shore oil wells and segmented shafts of motor vehicles. In this paper we shall study a model which may be applicable to long satellite antennae and booms which are segmented and collapsed during transport, and deployed in orbit (Hedgepeth, 1986). The satellite is also rotated for thermal and attitude stability reasons.

2. FORMULATION

We assume the originally straight rod is composed of N identical homogeneous links of length l and mass m. There are N linear torsion springs at the joints, each with a spring constant λ. Figure 1(a) shows a deformed shape in a plane rotating with the angular velocity Ω about the x' axis. Figure 1(b) shows the forces and moments on the nth link. Let the distances of the link tips from the rotation axis be b'_{n-1} and b'_n as shown. If we integrate along the link the total centrifugal force is

$$F'_n = m\Omega^2 (b'_{n-1} + b'_n)/2. \tag{1}$$

This force is located at a distance s'_n from one end:

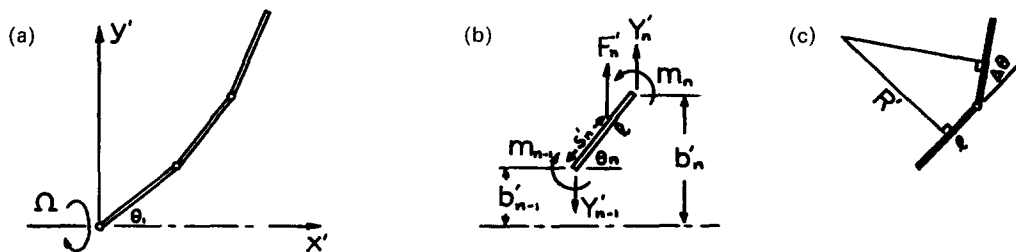$$s'_n = \frac{l}{3}(b'_{n-1} + 2b'_n)/(b'_{n-1} + b'_n). \tag{2}$$

Fig. 1. (a) Coordinate system; (b) balance on a single link; (c) equivalent radius R'.

Notice due to uneven centrifugal forces, the location of F'_n is not at the midpoint of the link. Let Y'_{n-1} and Y'_n be the forces at the ends. Equilibrium gives

$$F'_n + Y'_n = Y'_{n-1}. \tag{3}$$

A moment balance yields

$$F'_n S'_n \cos\theta_n + Y'_n l \cos\theta_n + M'_n = M'_{n-1}. \tag{4}$$

Here θ_n is the angle of inclination and M'_n is the moment from the torsion springs

$$M'_n = \lambda(\theta_{n+1} - \theta_n). \tag{5}$$

We normalize all lengths by the total length of the rod $L = Nl$, the forces by $l\lambda/L^2$ and drop primes. Equation (3) yields

$$Y_n = Y_{n-1} - \frac{B}{2N}(b_{n-1} + b_n), \tag{6}$$

where $B \equiv m\Omega^2 L^4/l^2\lambda$ is an important nondimensional parameter signifying the relative importance of centrifugal forces to the restoring forces of the springs. Equations (2), (4), (5) give

$$\theta_{n+1} = 2\theta_n - \theta_{n-1} - [Y_n/N^2 + B(b_{n-1} + 2b_n)/6N^3]\cos\theta_n. \tag{7}$$

Geometry also dictates that

$$b_n = b_{n-1} + \frac{1}{N}\sin\theta_n. \tag{8}$$

In order to facilitate the boundary conditions, fictitious links indexed $n = 0$ and $n = N+1$ are added. The boundary conditions are

$$\theta_0 = 0, \tag{9}$$

$$b_0 = 0, \tag{10}$$

$$Y_N = 0, \tag{11}$$

$$\theta_N = \theta_{N+1}. \tag{12}$$

The last condition indicates the free end is moment free. The nonlinear set of difference equations [eqns (6)–(12)] are to be solved for given N and B, with $n = 1$ to N.

3. BIFURCATION

In order to determine the critical rotation speeds B_c where the solution bifurcates from the trivial (straight) one, eqns (7), (8) are linearized for small θ_n

$$\theta_{n+1} = 2\theta_n - \theta_{n-1} - Y_n/N^2 - B_c(b_{n-1} + 2b_n)/6N^3, \tag{13}$$

$$b_n = b_{n-1} + \theta_n/N. \tag{14}$$

Table 1. Critical speeds B_c for $N \leqslant 6$

N	B_c					
1	3.00000					
2	5.45383	241.403				
3	6.92924	297.090	2144.67			
4	7.89536	327.741	2614.19	8483.1		
5	8.57307	349.542	2806.24	10480.3	23244.2	
6	9.07359	366.063	2928.58	11268.8	28939.8	51583.9

Together with eqns (6), (9)–(12) there are $3N$ unknowns and $3N$ homogeneous equations. The number of unknowns can be reduced by eliminating Y_i and b_i as follows. Increase n in eqns (6), (13) and use eqn (14) to obtain

$$\theta_{n+2} - 3\theta_{n+1} + 3\theta_n - \theta_{n-1} = \frac{B_c}{6N^3}[6b_{n-1} + (\theta_{n+1} + 5\theta_n)/N]. \tag{15}$$

Increasing n and removing b_i from eqn (14) gives an equation in θ_i

$$\theta_{n+3} - 4\theta_{n+2} + 6\theta_{n+1} - 4\theta_n + \theta_{n-1} - B_c(\theta_{n+2} + 4\theta_{n+1} + \theta_n)/6N^4 = 0, \quad n = 1 \text{ to } N-2. \tag{16}$$

The boundary condition $b_0 = 0$ is obtained from eqn (15)

$$\theta_3 - 3\theta_2 + 3\theta_1 - B(\theta_2 + 5\theta_1)/6N^4 = 0. \tag{17}$$

Setting $n = N-1$ in eqn (15) and using eqn (14) yield

$$\theta_{N+1} - 3\theta_N + 3\theta_{N-1} - \theta_{N-2} = \frac{B_c}{6N^3}[6b_N - (\theta_{N-1} + 5\theta_N)/N]. \tag{18}$$

Similarly

$$\theta_N - 3\theta_{N-1} + 3\theta_{N-2} - \theta_{N-3} = \frac{B_c}{6N^3}[6b_{N-1} - (\theta_{N-2} + 5\theta_{N-1})/N]. \tag{19}$$

Setting $n = N$ in eqn (13) and using eqns (11), (12), (18), (19) the boundary condition $Y_N = 0$ becomes

$$-9\theta_N + 9\theta_{N-1} + \theta_{N-2} - \theta_{N-3} + B_c(\theta_{N-2} + 7\theta_{N-1} + 10\theta_N)/6N^4 = 0. \tag{20}$$

Equations (16), (17), (20) are a set of N equations and N unknowns ($N \geqslant 3$). For eigenvalues B_c, the determinant of coefficients of θ_i is set to zero.

For the one link case ($N = 1$), eqns (13), (14) yield the eigenvalue $B = 3$. For $N = 2$ eqns (6), (13), (14) give $B_c = 96(9 \pm \sqrt{74})/7$. The two roots correspond to the two possible deformation modes. For $N \geqslant 3$ the determinant is solved numerically. Table 1 shows the results for $N \leqslant 6$. There are N possible modes of bifurcation.

4. RELATION BETWEEN THE SEGMENTED ROD AND THE CONTINUOUS ROD

For fixed L as $N \to \infty$ we expect that the segmented rod asymptotically approaches a continuous rod. Define a local radius of curvature R' as in Fig. 1(c):

Table 2. Critical speeds for the first three modes, large N

N	$B_c^{1/4}$		
5	1.7111	4.3239	7.2783
10	1.7877	4.4868	7.5246
15	1.8155	4.5502	7.6220
20	1.8299	4.5840	7.6751
25	1.8387	4.6049	7.7085
40	1.8521	4.6373	7.7610
100	1.8659	4.6709	7.8160
$J_c(N = \infty)$	1.8751	4.6941	7.8548

$$R' = \frac{l}{2}\cot\left(\frac{\Delta\theta}{2}\right). \tag{21}$$

Define flexural rigidity EI as the ratio of local moment to local curvature. As $\Delta\theta \to 0$

$$EI = \frac{\lambda\Delta\theta}{1/R'} \approx \lambda L/N. \tag{22}$$

In terms of EI our parameter B is then equivalent to J^4 in the continuous case (Wang, 1982):

$$B = \rho\Omega^2 L^4/EI = J^4, \tag{23}$$

where ρ is the density. From previous work, the infinite number of eigenspeeds for the stability of a rotating elastic rod are governed by the characteristic equation

$$1 + \cosh J_c \cos J_c = 0, \tag{24}$$

where we find $J_c = 1.87510, 4.69409, 7.85476, \ldots$. Table 2 shows the asymptotic approach of $B_c^{1/4}$ towards J_c for the first three eigenvalues. We see that when a segmented rod is approximated by a continuous one, the number of segments must be over 40 for 5% error, and N must be over 100 for 1% error.

5. NUMERICAL SOLUTION OF THE NONLINEAR PROBLEM

For large θ_n, a numerical solution of eqns (6)–(12) is necessary. For given N and $B > B_c$, we guess θ_1 and Y_0. The system, eqns (6)–(10), then generates sequences b_n, Y_n, θ_n. Set

$$u = Y_N, \quad v = \theta_N - \theta_{N+1}. \tag{25}$$

The problem is equivalent to solving the nonlinear equations of two unknowns

$$u(\theta_1, Y_0) = 0, \quad v(\theta_1, Y_0) = 0. \tag{26}$$

The functions u, v generated by nonlinear difference equations, are very difficult to solve, even numerically. We note that the solutions are bounded by $0 \leqslant \theta_1 \leqslant \pi/2$ and $0 \leqslant Y_0 \leqslant B/2$, with the upper bound obtained by considering the extreme case of $\theta_i = \pi/2$, $i \neq 0$. The possible locations of the roots can then be visualized by the minima of the scalar field
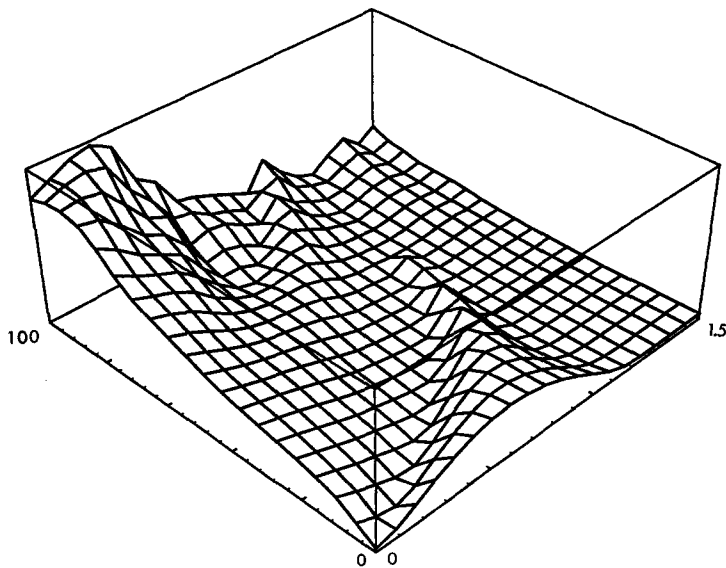
Fig. 2. Topography of S for $B = 200$. Left and right axes are Y_0 and θ_1, respectively.

$$S(\theta_1, Y_0) = u^2 + v^2. \tag{27}$$

Figure 2 shows the topography of S when $N = 6$ and $B = 200$. When B is increased to 400 the peaks become more jagged as seen in Fig. 3. By gradually refining the mesh we find the lowest points are in a basin near the top corner and along a slender trench left of the right ridge. A root finding scheme then yields two nontrivial solutions for θ_1 and Y_0 corresponding to the first and second bifurcation modes. Figure 4 shows the configurations for $B = 400$ and $N = 6$. We emphasize here that the topographical map of S is extremely helpful in locating the roots.

6. RESULTS AND DISCUSSION

For large values of B the solutions are nonunique. In what follows we shall concentrate on the more important first mode. The moment at the base (normalized by λ) is represented
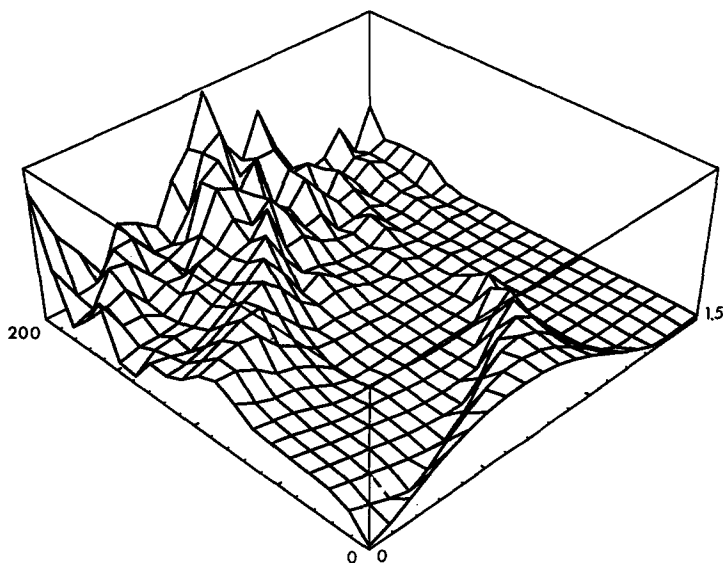

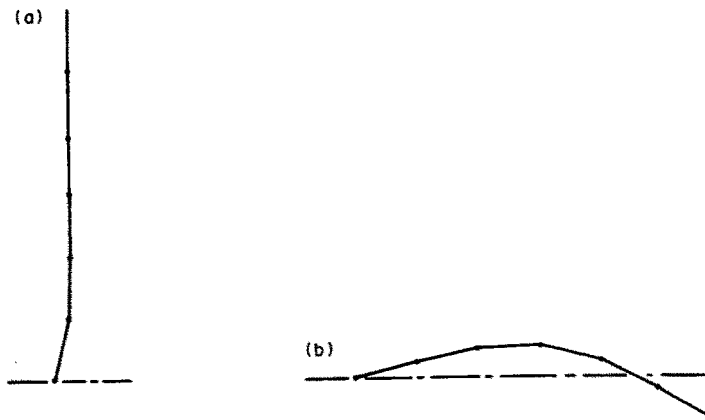
Fig. 3. Topography of S for $B = 400$.

Fig. 4. Two solutions for $B = 400$, $N = 6$. (a) First mode ($\theta_1 = 1.355$, $Y_0 = 198.56$). (b) Second mode ($\theta_1 = 0.2453$, $Y_0 = 10.18$).

by θ_1. Figure 5 shows θ_1 for the first mode as a function of B at various constants N. The one-link case ($N = 1$) is obtained by the inverse relation

$$B = \frac{6\theta_1}{\sin 2\theta_1}, \quad Y_0 = \frac{B}{2}\sin\theta_1. \tag{28}$$

All curves bifurcate from B_c given in Table 1 and increase monotonically, approaching $\pi/2$ as $B \to \infty$. The rate of increase is slower for larger N. As $N \to \infty$, $\theta_1 \to 0$. The maximum force at the base Y_0 is plotted in Fig. 6. The curves are asymptotic to $B/2$ for large B. Also shown is the continuous case ($N = \infty$) from Wang (1982). Figures 5 and 6 should be useful for design purposes.

Some deformed configurations are shown in Fig. 7. For fixed N the displacements are larger for larger B or rotation rate. However, for fixed B the displacements are smaller for larger N. This is also reflected in the stability analysis, where B_c becomes larger as N is increased. The conclusion that more segments imply more stability is of course erroneous.
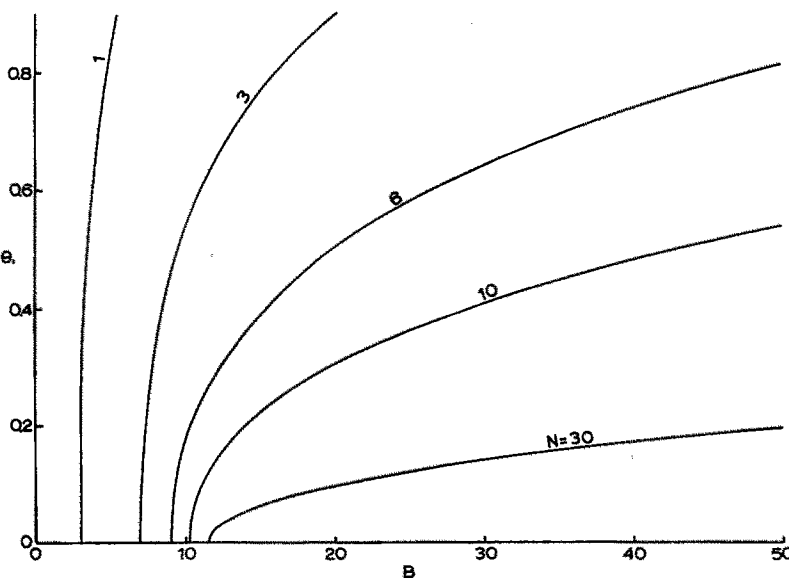

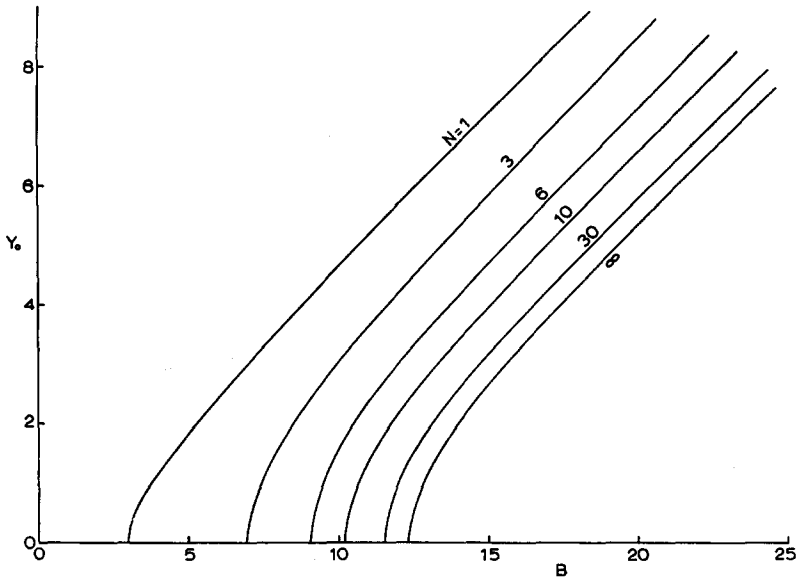Fig. 5. Maximum normalized moment or θ_1 for the first mode.

Fig. 6. Maximum normalized force or Y_0, first mode.

If total length L, total mass M and spring constant λ are all fixed, we find

$$B = \frac{NM\Omega^2 L^2}{\lambda} \tag{29}$$

and thus the critical speed is represented by B/N instead. We see from Table 1 the value of B_c/N decreases as N is increased. Thus for fixed total dimensions more segments imply less stability.

Mathematically, the discrete segmented rod presents a more difficult problem than the continuous elastica rod. The nonlinear difference equations in this paper cannot be similarly analysed for existence as the nonlinear differential equations of the elastica. Also stretching transforms are not valid in the present discrete case. For example, boundary layer theory for large rotation rates (Wang, 1982) is not applicable here. Again due to the lack of stretching transforms, tedious numerical schemes are necessary for obtaining the nonunique solutions. In contrast, the numerical integration for the continuous case can be reduced by stretching transforms to a one parameter shooting algorithm.

In other applications, models of rotating segmented rods may differ in the governing equations or the boundary conditions. This paper illustrates some possible methods to treat the resulting nonlinear difference equations.
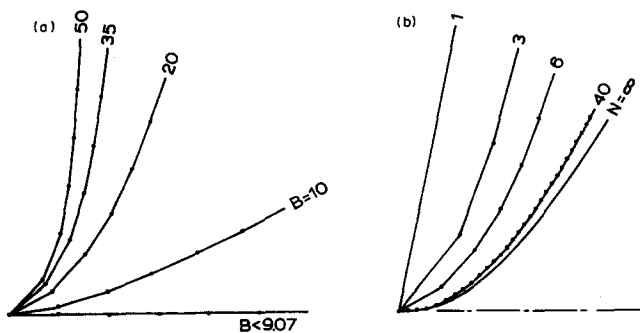

Fig. 7. Deformed configurations. (a) $N = 6$ as B is varied. (b) $B = 20$ as N is varied.

REFERENCES

Atanackovic, T. M. (1984). Estimates of maximum deflection for a rotating rod. *Q. J. Mech. Appl. Math.* **37**, 515–523.

Hedgepeth, J. M. (1986). Conceptual design of deployable truss structures. *Proc. 10th U.S. Nat. Congr. Appl. Mech.*, Austin, Texas.

Love, A. E. H. (1944). *Mathematical Theory of Elasticity* (4th Edn). Dover, New York.

Odeh, F. and Tadjbakhsh, I. (1965). A nonlinear eigenvalue problem for rotating rods. *Arch. Rat. Mech. Anal.* **20**, 81–94.

Wang, C. Y. (1982). On the bifurcation solutions of an axially rotating rod. *Q. J. Mech. Appl. Math.* **35**, 391–402.